JACS
JOURNAL OF THE AMERICAN CHEMICAL SOCIETY

COMMUNICATION

pubs.acs.org/JACS

Selective Enhancement of Nucleases by Polyvalent DNA-Functionalized Gold Nanoparticles

Andrew E. Prigodich, Ali H. Alhasan, and Chad A. Mirkin*

Department of Chemistry and International Institute of Nanotechnology, Northwestern University, Evanston, Illinois 60208, United States

Supporting Information

ABSTRACT: We demonstrate that polyvalent DNA-functionalized gold nanoparticles (DNA-Au NPs) selectively enhance ribonuclease H (RNase H) activity while inhibiting most biologically relevant nucleases. This combination of properties is particularly interesting in the context of gene regulation, since high RNase H activity results in rapid mRNA degradation and general nuclease inhibition results in high biological stability. We have investigated the mechanism of selective RNase H activation and found that the high DNA density of DNA-Au NPs is responsible for this unusual behavior. This work adds to our understanding of polyvalent DNA-Au NPs as gene regulation agents and suggests a new model for selectively controlling protein−nanoparticle interactions.

The relationship between a material's nanostructure and its interactions with biomolecules represents an important area of research. The promise of this research lies in the ability to selectively engage specific molecules in complex biological environments, which could potentially lead to more accurate diagnostics and more potent therapeutics.[1] The interactions between oligonucleotides and nucleases (enzymes that degrade nucleic acids) are particularly important because they play a central role in gene detection and regulation.[2] Unmodified oligonucleotides are rapidly destroyed by nonspecific nucleases in most biological environments, rendering them less effective. Chemists have developed designer nucleic acids to combat this problem by retarding nuclease-catalyzed degradation.[3] This leads to greater oligonucleotide stability but can have unintended consequences, as some nucleases are necessary for biological applications. For example, messenger RNA (mRNA) expression can be regulated by antisense oligonucleotides through interactions with ribonuclease H (RNase H), but in this case, designer nucleic acids are counterproductive, inhibiting RNase H and leading to ineffective gene knockdown.[2] This problem is generally overcome through a compromise in which oligonucleotides containing both designer and traditional nucleic acid regions are used. These chimeric molecules have enhanced stability and some RNase H reactivity but do not maximize either, leading to the desire to create a single agent that inhibits nonspecific nucleases but also selectively enhances the activity of RNase H.

DNA-functionalized gold nanoparticles (DNA-Au NPs) are efficient agents in many applications, including materials assembly,[4] detection,[5] and gene regulation.[6] These nanoparticles have many attributes that make them ideal for these applications, including distance-dependent optical properties,[7] efficient programmable binding,[5e,8] rapid cell uptake,[9] and little innate immune response,[10] but biological stability stemming from the nuclease-resistant cloud of concentrated DNA and salt surrounding each nanoparticle is particularly important.[11] Despite this general nuclease inhibition, DNA-Au NPs are effective gene regulation agents, acting through the RNase H pathway.[6d] Although these DNA-Au NPs have been well-studied, their combination of potent gene regulation and nuclease inhibition is both practically important and scientifically surprising. In view of this, we chose to directly investigate RNase H activity on DNA-Au NPs. We report that in contrast to most nucleases studied to date, RNase H activity is enhanced on the nanoparticle surface, making DNA-Au NPs ideal gene regulation agents, as they are both highly stable in biological environments and highly active in the presence of target mRNA (Figure 1).

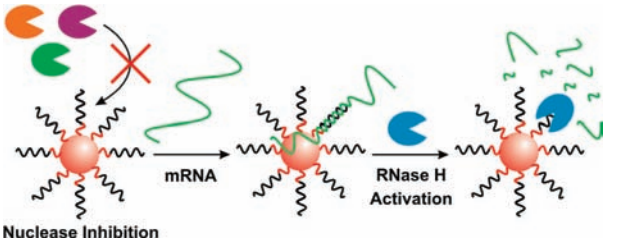

Figure 1. Schematic representation of general nuclease inhibition and RNase H activation by DNA-Au NPs. The Au NP, depicted as a red sphere, is functionalized with DNA. The recognition region of the DNA is depicted in black, and the A10-thiol spacer linking the target region to the gold surface is depicted in red. Most nucleases (shown at the far left in orange, purple, and green) are inhibited by the nanoparticle surface, leading to high stability for the DNA-Au NPs. Once target mRNA (green line) binds to the nanoparticle, enhanced RNase H (right side, blue) catalysis at the nanoparticle surface leads to rapid RNA degradation and efficient gene regulation.

The first step in this investigation was to create a model RNase H substrate containing a fluorophore-labeled RNA/DNA heteroduplex. This was accomplished by hybridizing fluorophore-labeled RNA to either Dabcyl-DNA (free target) or DNA-Au NPs. Similar substrates were created to compare RNase H to deoxyribonuclease I (DNase I) and serum nucleases. The number of DNA molecules per nanoparticle was measured using a commercial assay (Invitrogen, Quant-It Oligreen).[9] In the intact substrate,

Received: December 2, 2010
Published: January 26, 2011

dx.doi.org/10.1021/ja110833r | J. Am. Chem. Soc. 2011, 133, 2120–2123

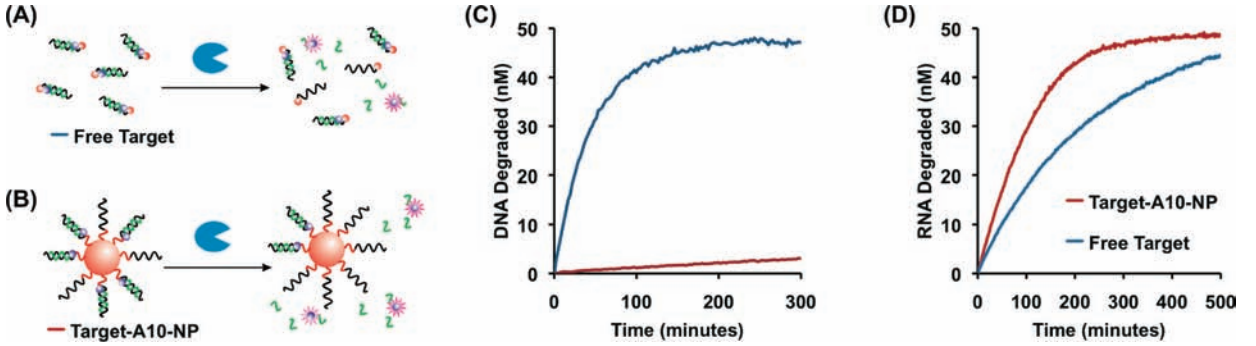

Figure 2. Comparison of RNase H and serum nuclease activities. (A, B) General schematic representations of the fluorescence-based degradation assays using (A) free and (B) nanoparticle-bound target. DNA, RNA, and nuclease are depicted in black, green, and blue respectively. The molecular quenchers (small orange circles) and excited fluorophores (pink stars) are also shown. (C, D) Progress curves of nucleic acid degradation are shown for (C) nonspecific serum nucleases and (D) RNase H. In each plot, the reaction rates of free substrate (blue) and nanoparticle-bound substrate (red) are compared. Each curve represents the average of three independent experiments.

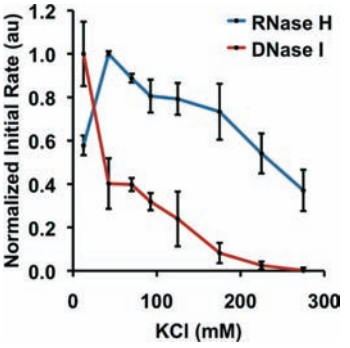

Figure 3. Salt sensitivity of RNase H (blue) and DNase I (red). Each point represents the normalized initial rate of substrate degradation; the errors bars represent standard errors from three independent experiments.

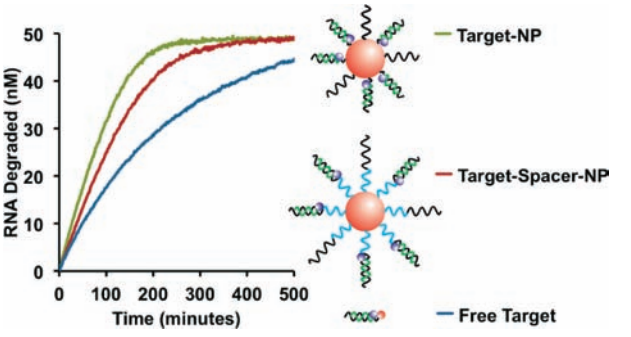

Figure 4. Effect of local substrate density on the reaction rate. Progress curves for three substrates were compared: free target (blue), target bound to a Au NP through a P10 spacer (red), and target bound directly to the Au NP surface (green). A schematic diagram of each substrate is shown, with the position of the spacer highlighted in blue. As in previous schemes, DNA and RNA are depicted in black and green respectively. Each curve represents the average of three independent experiments.

the proximity of the fluorophore to the quencher (either the NP or Dabcyl) resulted in distance-dependent quenching. When the substrate was exposed to the appropriate nuclease, the nucleic acid was degraded, resulting in release of the fluorophore, which could be monitored in real time as an increase in solution-associated fluorescence (Figure 2A,B).

The activities of serum nucleases on DNA-Au NPs and free DNA substrates were compared using the materials described above and established protocols (Figure 1).[11b] Consistent with previous results,[11a] serum nucleases were strongly inhibited by the nanoparticle conjugate (Figure 2C). RNase H was tested (Figure 2D), and surprisingly, RNase H exhibited 2.5 ± 0.1 times faster degradation on the polyvalent oligonucleotide-functionalized nanoparticle relative to the same substrate free in solution. This preferential interaction of RNA/DNA-Au NPs with RNase H explains why these nanoparticles are active in RNase H-mediated gene regulation while degradation by other nucleases is still prevented.

In order to investigate the surprising activity of RNase H on polyvalent DNA-Au NPs, we looked at the enzyme's salt tolerance, because DNA-Au NPs inhibit general nucleases through the high local salt concentration around the nanoparticle surface.[11b] The effects of salt concentration on the degradation of free substrates by RNase H and DNase I, a well-studied model nuclease, were compared. The initial reaction rates for each enzyme were determined and plotted as a function of KCl concentration (Figure 3). RNase H is clearly more active than DNase I under high-KCl conditions; for example, RNase H is 20-fold faster than DNase I at 225 mM KCl. Similar results were observed using NaCl (Figure S1 in the Supporting Information). The salt tolerance of RNase H explains its lack of inhibition by nanoparticles, but it does not fully explain the observed increase in activity (Figure 2D).

To further explore nanoparticle−RNase H interactions, we investigated the role of local DNA density, which is much higher on the polyvalent DNA-Au NP surface than with conventional oligonucleotides. The first step was to synthesize nanoparticles with different DNA densities by changing the distance between the Au NP and the DNA. DNA-Au NPs were made with the DNA either bound directly to the nanoparticle surface or bound through a 10-unit propyl phosphodiester spacer (P10) (Figure 4). Without the spacer, the DNA was ~2.2 times more dense because of the radius of curvature of the nanoparticle (calculated on the basis of previous results;[12] see the Supporting Information). The increase in density led to an increase in RNase H activity from 0.25 ± 0.01 to 0.46 ± 0.03 to 0.68 ± 0.04 h^{-1} for free targets, moderate-density NPs, and high-density NPs, respectively (Figure 4). These results were confirmed with nanoparticles containing different spacer compositions (Figures S2 and S3). The correlation

dx.doi.org/10.1021/ja110833r |J. Am. Chem. Soc. 2011, 133, 2120–2123

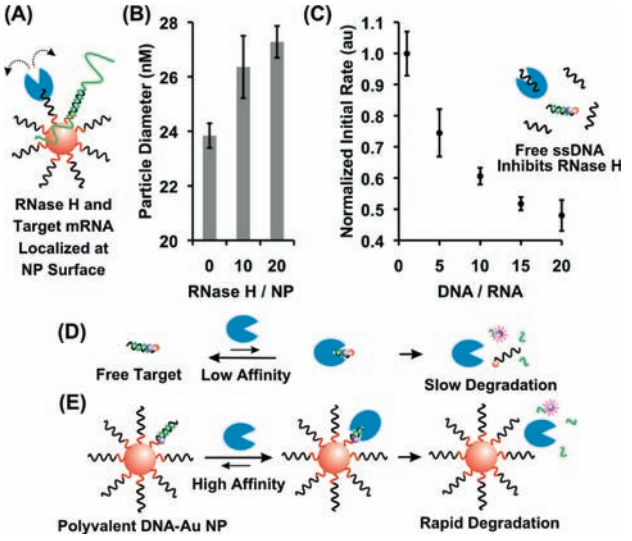

Figure 5. High DNA density localizes RNase H near its target. (A) Proposed intermediate having RNase H and target bound to the NP. (B) DLS measurements of particle diameters at multiple RNase H concentrations. (C) RNase H inhibition by ssDNA not bound to nanoparticles. Each point represents the normalized initial rate of substrate degradation. The error bars represent standard errors from three independent experiments. (D, E) Schematic of (D) free and (E) nanoparticle-bound substrates. As in previous schemes, DNA, RNA, and RNase H are depicted in black, green, and blue, respectively.

between high local target concentration and high RNase H activity indicates that steric hindrance is not a major issue under the conditions tested.

Since RNase H is known to associate with single-stranded DNA (ssDNA),[13] we hypothesized that the relatively high DNA density increases the RNase H activity by binding and localizing the enzyme at the nanoparticle surface, positioning it in close proximity to its target (Figure 5).[14] To test this, the RNase H affinities for DNA-Au NPs and free target were quantitatively compared by a Michaelis–Menten analysis. The measured Michaelis constant (K_M) for the nanoparticle was enhanced by ~2-fold relative to the free duplex, indicating that the rapid reaction rates on the nanoparticle are at least in part the result of the relatively high affinity between the enzyme and the DNA-Au NP (Figure S4). This is consistent with RNase H localization at the nanoparticle surface due to polyvalent ssDNA interactions, but K_M analysis does not directly address the role of ssDNA (Figure 5A). To confirm that RNase H associates with ssDNA-Au NPs even without target RNA, the system was studied by dynamic light scattering (DLS) (Figure 5B). The particle diameter increased by 2.5 ± 0.3 nm in the presence of excess RNase H, consistent with RNase H binding.[15] Again, this is consistent with the polyvalent ssDNA surface localizing RNase H near its RNA/DNA substrate. To confirm that ssDNA polyvalency is critical for the observed increase in rate, we investigated the effect of excess ssDNA on free-duplex degradation (Figure 5C). In this case, ssDNA inhibited rather than facilitated the reaction, likely because the free ssDNA was not localized near the DNA/RNA target and thus competed for RNase H binding. Similar experiments were performed on the nanoparticle-bound system to further support this finding (Figure S5). Taken together, these results support the proposed mechanism of enhanced RNase H activity, in which enzyme–target association is facilitated by the localization of both RNase H and its RNA target in close proximity at the nanoparticle surface. This is not observed for other nucleases, most likely because they are inhibited by the high local salt concentration, which is present in high DNA density environments. As a result, increasing DNA density can be used to specifically increase RNase H activity while simultaneously decreasing degradation by other nucleases.

Polyvalent DNA-Au NPs are highly stable in biological environments because most nucleases are inhibited by the high local salt concentration around the nanoparticle surface.[11] This makes them excellent agents for many applications, including gene regulation.[6b] However, DNA-Au NPs require a nuclease, RNase H, to engage the gene regulation pathway. This apparent inconsistency has been resolved; unlike other nucleases, RNase H activity is enhanced by the DNA-Au NP (Figure 2). We have identified two biochemical properties that help explain this surprising observation. First, RNase H is a particularly salt-tolerant nuclease, and as such, it is relatively unperturbed by the high-salt environment of the nanoparticle (Figure 3). Second, the high DNA density on the nanoparticle surface leads to higher reaction rates, likely as a result of the high effective substrate concentration around the nanoparticle surface (Figures 4 and 5). These features make DNA-Au NPs both highly stable in biological environments and highly active in the RNase H-based gene regulation pathway. This work not only accounts for the remarkable utility of polyvalent DNA-Au NPs but also establishes a nanochemistry-based method for selectively activating a specific enzyme while simultaneously inhibiting closely related enzymes. It thus represents a significant step toward creating programmable nanoparticle–protein interactions.

■ ASSOCIATED CONTENT

Supporting Information. Supporting figures, experimental methods, and calculations. This material is available free of charge via the Internet at http://pubs.acs.org.

■ AUTHOR INFORMATION

Corresponding Author
chadnano@northwestern.edu

■ ACKNOWLEDGMENT

This material is based upon work supported by the DARPA US Army RDECOM Acquisition Center under Award No. W911NF-09-1-0069 and W81XWH-08-1-0766. Additionally, the project was supported by Award Numbers U54CA151880 and U54CA119341 from the National Cancer Institute. A.E.P. and A.H.A. acknowledge the Ryan Fellowship and the K.S.A. King Abdullah Scholarship, respectively.

■ REFERENCES

(1) (a) Niemeyer, C. M. *Angew. Chem., Int. Ed.* **2001**, *40*, 4128–4158. (b) Kim, J.; Grate, J. W.; Wang, P. *Chem. Eng. Sci.* **2006**, *61*, 1017–1026. (c) Rosi, N. L.; Mirkin, C. A. *Chem. Rev.* **2005**, *105*, 1547–1562. (d) Giljohann, D. A.; Mirkin, C. A. *Nature* **2009**, *462*, 461–464. (e) Chen, C. L.; Rosi, N. L. *Angew. Chem., Int. Ed.* **2010**, *49*, 1924–1942.

(2) (a) Akhtar, S.; Hughes, M. D.; Khan, A.; Bibby, M.; Hussain, M.; Nawaz, Q.; Double, J.; Sayyed, P. *Adv. Drug Delivery Rev.* **2000**, *44*, 3–21. (b) Crooke, S. T. *Annu. Rev. Med.* **2004**, *55*, 61–95.

(3) (a) Petersen, M.; Wengel, J. *Trends Biotechnol.* **2003**, *21*, 74–81. (b) Shangguan, D.; Tang, Z. W.; Mallikaratchy, P.; Xiao, Z. Y.; Tan, W. H. *ChemBioChem* **2007**, *8*, 603–606.

(4) (a) Mirkin, C. A.; Letsinger, R. L.; Mucic, R. C.; Storhoff, J. J. *Nature* **1996**, *382*, 607–609. (b) Alivisatos, A. P.; Johnsson, K. P.; Peng, X. G.; Wilson, T. E.; Loweth, C. J.; Bruchez, M. P.; Schultz, P. G. *Nature* **1996**, *382*, 609–611. (c) Park, S. Y.; Lytton-Jean, A. K. R.; Lee, B.; Weigand, S.; Schatz, G. C.; Mirkin, C. A. *Nature* **2008**, *451*, 553–556. (d) Nykypanchuk, D.; Maye, M. M.; van der Lelie, D.; Gang, O. *Nature* **2008**, *451*, 549–552.

(5) (a) He, L.; Musick, M. D.; Nicewarner, S. R.; Salinas, F. G.; Benkovic, S. J.; Natan, M. J.; Keating, C. D. *J. Am. Chem. Soc.* **2000**, *122*, 9071–9077. (b) Liu, J. W.; Lu, Y. *J. Am. Chem. Soc.* **2003**, *125*, 6642–6643. (c) Nam, J. M.; Thaxton, C. S.; Mirkin, C. A. *Science* **2003**, *301*, 1884–1886. (d) Seferos, D. S.; Giljohann, D. A.; Hill, H. D.; Prigodich, A. E.; Mirkin, C. A. *J. Am. Chem. Soc.* **2007**, *129*, 15477–15479. (e) Prigodich, A. E.; Lee, O. S.; Daniel, W. L.; Seferos, D. S.; Schatz, G. C.; Mirkin, C. A. *J. Am. Chem. Soc.* **2010**, *132*, 10638–10641.

(6) (a) Agbasi-Porter, C.; Ryman-Rasmussen, J.; Franzen, S.; Feldheim, D. *Bioconjugate Chem.* **2006**, *17*, 1178–1183. (b) Rosi, N. L.; Giljohann, D. A.; Thaxton, C. S.; Lytton-Jean, A. K. R.; Han, M. S.; Mirkin, C. A. *Science* **2006**, *312*, 1027–1030. (c) Liu, Y. L.; Franzen, S. *Bioconjugate Chem.* **2008**, *19*, 1009–1016. (d) Prigodich, A. E.; Seferos, D. S.; Massich, M. D.; Giljohann, D. A.; Lane, B. C.; Mirkin, C. A. *ACS Nano* **2009**, *3*, 2147–2152. (e) Giljohann, D. A.; Seferos, D. S.; Daniel, W. L.; Massich, M. D.; Patel, P. C.; Mirkin, C. A. *Angew. Chem., Int. Ed.* **2010**, *49*, 3280–3294.

(7) (a) Storhoff, J. J.; Lazarides, A. A.; Mucic, R. C.; Mirkin, C. A.; Letsinger, R. L.; Schatz, G. C. *J. Am. Chem. Soc.* **2000**, *122*, 4640–4650. (b) Zhu, M.; Aikens, C. M.; Hollander, F. J.; Schatz, G. C.; Jin, R. *J. Am. Chem. Soc.* **2008**, *130*, 5883–5885.

(8) (a) Huang, C. C.; Huang, Y. F.; Cao, Z. H.; Tan, W. H.; Chang, H. T. *Anal. Chem.* **2005**, *77*, 5735–5741. (b) Lytton-Jean, A. K. R.; Mirkin, C. A. *J. Am. Chem. Soc.* **2005**, *127*, 12754–12755.

(9) Giljohann, D. A.; Seferos, D. S.; Patel, P. C.; Millstone, J. E.; Rosi, N. L.; Mirkin, C. A. *Nano Lett.* **2007**, *7*, 3818–3821.

(10) Massich, M. D.; Giljohann, D. A.; Seferos, D. S.; Ludlow, L. E.; Horvath, C. M.; Mirkin, C. A. *Mol. Pharmaceutics* **2009**, *6*, 1934–1940.

(11) (a) Giljohann, D. A.; Seferos, D. S.; Prigodich, A. E.; Patel, P. C.; Mirkin, C. A. *J. Am. Chem. Soc.* **2009**, *131*, 2072–2073. (b) Seferos, D. S.; Prigodich, A. E.; Giljohann, D. A.; Patel, P. C.; Mirkin, C. A. *Nano Lett.* **2009**, *9*, 308–311.

(12) Macfarlane, R. J.; Jones, M. R.; Senesi, A. J.; Young, K. L.; Lee, B.; Wu, J. S.; Mirkin, C. A. *Angew. Chem., Int. Ed.* **2010**, *49*, 4589–4592.

(13) (a) Gopalakrishnan, V.; Peliska, J. A.; Benkovic, S. J. *Proc. Natl. Acad. Sci. U.S.A.* **1992**, *89*, 10763–10767. (b) Lima, W. F.; Wu, H. J.; Nichols, J. G.; Prakash, T. P.; Ravikumar, V.; Crooke, S. T. *J. Biol. Chem.* **2003**, *278*, 49860–49867.

(14) (a) Halford, S. E.; Marko, J. F. *Nucleic Acids Res.* **2004**, *32*, 3040–3052. (b) von Hippel, P. H. *Annu. Rev. Biophys. Biomol. Struct.* **2007**, *36*, 79–105.

(15) Katayanagi, K.; Miyagawa, M.; Matsushima, M.; Ishikawa, M.; Kanaya, S.; Ikehara, M.; Matsuzaki, T.; Morikawa, K. *Nature* **1990**, *347*, 306–309.